# Electromagnetically Induced Coherent Backscattering

Yuri V. Rostovtsev,[1] Zoe-Elizabeth Sariyanni,[1] and Marlan O. Scully[1,2,3]

[1]*Department of Physics and Institute for Quantum Studies, Texas A & M University, Texas 77843, USA*

[2]*Princeton Institute for the Science and Technology of Materials and Department of Mechanical & Aerospace Engineering, Princeton University, New Jersey 08544, USA*

[3]*Max-Planck-Institute für Quantenoptik, D-85748 Garching, Germany*

(Received 17 November 2005; published 14 September 2006)

We demonstrate a strong coherent backward wave oscillation using forward propagating fields only. This is achieved by applying laser fields to an ultradispersive medium with proper chosen detunings to excite a molecular vibrational coherence that corresponds to a backward propagating wave. The physics then has much in common with the propagation of ultraslow light. Applications to coherent scattering and remote sensing are discussed.

DOI: 10.1103/PhysRevLett.97.113001 PACS numbers: 32.80.Qk, 42.50.Hz, 42.65.Dr

Quantum coherence [1,2] has been shown to result in many counter-intuitive phenomena. The scattering via a gradient force in gases [3], the forward Brillouin scattering in ultradispersive resonant media [4,5], electromagnetically induced transparency [6–9], slow light [10–13], Doppler broadening elimination [14], light induced chirality in nonchiral medium [15], a new class of entanglement amplifier [16] based on correlated spontaneous emission lasers [17,18], and the coherent Raman scattering enhancement via maximal coherence in atoms [19] and biomolecules [20–22] are a few examples that demonstrate the importance of quantum coherence.

In this Letter, we predict strong coherent backward scattering via excitation of quantum coherence between atomic or molecular levels. The developed approach can also be used to control the direction of the signal generated in coherent Raman scattering and other four-wave mixing (FWM) schemes.

Let us consider the four-wave mixing in a 3-level atomic medium. The pump and Stokes fields $\mathcal{E}_1$ and $\mathcal{E}_2$ (whose Rabi frequencies are defined as $\Omega_1 = \wp_1\mathcal{E}_1/\hbar$ and $\Omega_2 = \wp_2\mathcal{E}_2/\hbar$, where $\wp_1$ and $\wp_2$ are the dipole moments of the corresponding transitions) with wave vectors $k_1$ and $k_2$ and angular frequencies $\nu_1$ and $\nu_2$ induce a coherence grating in the medium (see Fig. 1) given by [2]

$$\rho_{cb} \sim -\Omega_1\Omega_2^*. \tag{1}$$

Let us stress that the $\rho_{cb}$ coherence grating has an $\exp[i(k_1 - k_2)z]$ spatial dependence. In an ultradispersive medium (see Fig. 2) where fields propagate with a slow group velocity, the two copropagating fields have wave vectors given by

$$k_1 \simeq k_1(\omega_{ab}) + \frac{\partial k_1}{\partial \nu_1}(\nu_1 - \omega_{ab}) = \omega_{ab}/c + (\nu_1 - \omega_{ab})/V_g, \tag{2}$$

where $V_g$ is the group velocity of the first wave, $\omega_{ab}$ is the frequency of the transition between levels $a$ and $b$, and $k_2 = \nu_2/c$. Thus these two fields create a coherence grating in the medium with spatial phase determined by $k_1 - k_2 = \omega_{cb}/c + (\nu_1 - \omega_{ab})/V_g$ which depends strongly on the detuning $\delta = \nu_1 - \omega_{ab}$. By properly choosing the detuning, $\delta$, one can make $k_1 - k_2$ negative.

After the coherence $\rho_{bc}$ is induced in the medium, a probe field $\mathcal{E}_3$, with Rabi frequency $\Omega_3 = \wp_3\mathcal{E}_3/\hbar$ and wave vector $k_3$, scatters off that coherence to produce the

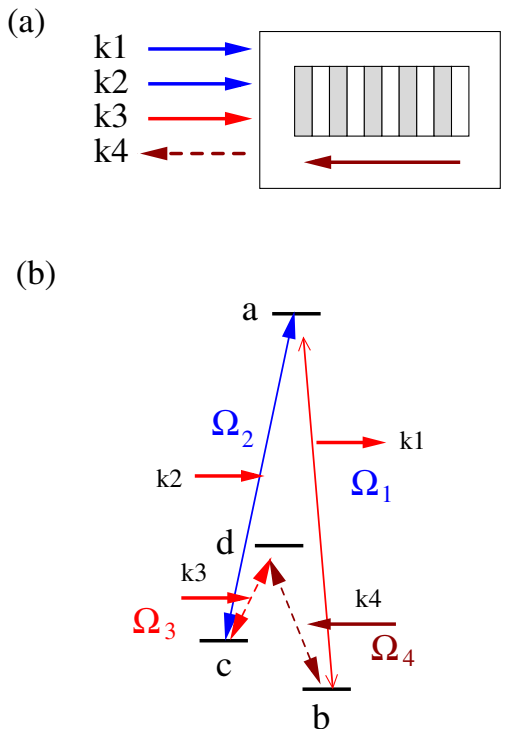


FIG. 1 (color online). (a) Copropagating fields 1 and 2 induce coherent grading inside the medium. The field 3 propagating in the same direction will be scattered in the opposite direction because the coherence excited by fields 1 and 2 is propagating in the opposite direction (see Fig. 2). Level scheme, double $\Lambda$ (b), for implementation of coherent backscattering.

 

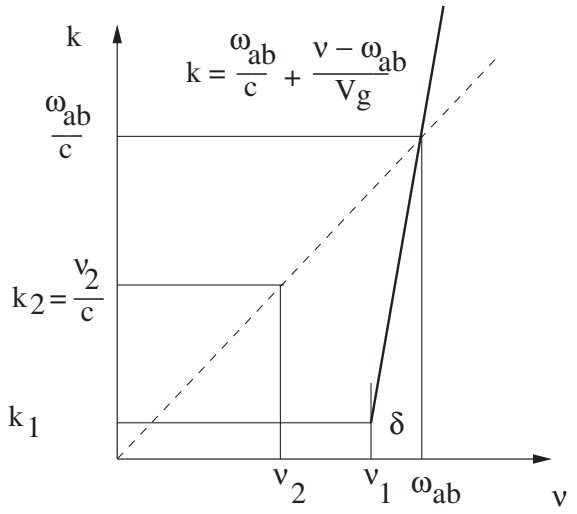


FIG. 2. Dispersion $k(\nu)$ of ultradispersive medium. Choosing $\delta = \nu_1 - \omega_{ab} = -V_g\omega_{cb}/c$, we can have $k_1 - k_2 < 0$ even if $\nu_1 > \nu_2$, thus the third field can be scattered opposite to the direction of propagation of the first two fields.

signal field, $\Omega_4$. The signal field depends on the coherence and the input fields as

$$\frac{\partial}{\partial z}\Omega_4 \sim \rho_{cb}\Omega_3 \sim \Omega_1\Omega_2^*\Omega_3 \sim e^{i(k_1-k_2+k_3-k_4)z}. \quad (3)$$

That is, the propagation direction of $\Omega_4$ depends on the spatial phase of the $\rho_{bc}$ coherence through the phase-matching condition $k_4 = k_1 - k_2 + k_3$ [23] while its frequency is determined by $\nu_4 = \nu_1 - \nu_2 + \nu_3$.

We here show that for dispersive media one can obtain a strong signal in the backward direction even when all three input fields propagate forward. This is contrary to the usual nondispersive media results, where the phase matching in the backward direction cannot be achieved for $\mathcal{E}_1$, $\mathcal{E}_2$, and $\mathcal{E}_3$ counterpropagating with respect to $\mathcal{E}_4$ [23].

To demonstrate this result, we write the interaction Hamiltonian of the system as

$$V_I = -\hbar[\Omega_1 e^{-i\omega_{ab}t}|a\rangle\langle b| + \Omega_2 e^{-i\omega_{ac}t}|a\rangle\langle c| + \text{H.c.}] \quad (4)$$

$$-\hbar[\Omega_4 e^{-i\omega_{db}t}|d\rangle\langle b| + \Omega_3 e^{-i\omega_{dc}t}|d\rangle\langle c| + \text{H.c.}], \quad (5)$$

where $\Omega_4 = \wp_4\mathcal{E}_4/\hbar$ is the Rabi frequency of the signal field and $\omega_{ab}$, $\omega_{ac}$, $\omega_{db}$, $\omega_{dc}$ are the frequency differences between the corresponding atomic or molecular energy levels [see Fig. 1(b)]. The time-dependent density matrix equations are given by

$$\frac{\partial\rho}{\partial\tau} = -\frac{i}{\hbar}[V_I, \rho] - \frac{1}{2}(\Gamma\rho + \rho\Gamma), \quad (6)$$

where $\Gamma$ is the relaxation matrix. A self-consistent system also includes the field propagation equations

$$\frac{\partial\Omega_1}{\partial z} + ik_1\Omega_1 = -i\eta_1\rho_{ab}, \qquad \frac{\partial\Omega_2}{\partial z} + ik_2\Omega_2 = -i\eta_2\rho_{ac}, \quad (7)$$

$$\frac{\partial\Omega_4}{\partial z} + ik_4\Omega_4 = -i\eta_3\rho_{db}, \qquad \frac{\partial\Omega_3}{\partial z} + ik_3\Omega_3 = -i\eta_4\rho_{dc}, \quad (8)$$

where $\eta_j = \nu_j N\wp_j^2/(2\epsilon_0 c\hbar)$ are the coupling constants ($j = 1, 2, 3, 4$), $N$ is the particle density of the medium, $\epsilon_0$ the permitivity in vacuum.

The equations of motion for the density matrix elements of the polarization $\rho_{ab}$ and the coherence $\rho_{cb}$ are given by

$$\dot{\rho}_{ab} = -\Gamma_{ab}\rho_{ab} + i\Omega_1(\rho_{aa} - \rho_{bb}) - i\rho_{cb}\Omega_2^*, \quad (9)$$

$$\dot{\rho}_{cb} = -\Gamma_{cb}\rho_{cb} + i\rho_{ca}\Omega_1 - i\rho_{ab}\Omega_2, \quad (10)$$

where $\Gamma_{ab} = \gamma_{ab} + i(\omega_{ab} - \nu_1)$; $\Gamma_{ca} = \gamma_{ca} - i(\omega_{ac} - \nu_2)$; $\Gamma_{cb} = \gamma_{cb} + i(\omega_{cb} - \nu_1 + \nu_2)$; $\omega_{cb}$ is the frequency of $c - b$ transition, and $\gamma_{\alpha\beta}$ are the relaxation rates at the corresponding transitions. The equation for $\rho_{ca}$ is obtained similarly to Eq. (9). In the steady-state regime, and assuming that $|\Omega_2| \gg |\Omega_1|$, almost all of the population remains in the ground level $|b\rangle$, $\rho_{bb} \simeq 1$. Let us consider the fields as plane waves: $\Omega_1(z, t) = \tilde{\Omega}_1(z, t)\exp(ik_1 z)$, $\Omega_2(z, t) = \tilde{\Omega}_2(z, t)\exp(ik_2 z)$, where $\tilde{\Omega}_1(z, t)$ and $\tilde{\Omega}_2(z, t)$ are the slowly varying in envelopes of the fields $\Omega_1$ and $\Omega_2$ in space, while $k_1 = \nu_1[1 + \frac{\chi_{ab}(\nu_1)}{2}]/c$ and $k_2 = \nu_2[1 + \frac{\chi_{ac}(\nu_2)}{2}]/c$. The susceptibilities are $\chi_{ab} = \eta_1\rho_{ab}/\Omega_1 = 2c(\nu_1 - \omega_{ab})/(\nu_1 V_g)$ and $\chi_{ac} = \eta_2\rho_{ac}/\Omega_2 \simeq 0$. By solving the self-consistent system of Maxwell's Eqs. (7) and (8), and the density matrix Eqs. (9) and (10), we obtain Eq. (2) for the wave vectors, where $V_g \simeq c|\Omega_2|^2/(\nu_1\eta_1)$ is the group velocity of the optical field $\Omega_1$. Thus, the spatial dependence of $\rho_{cb}$ is determined by

$$\Delta k = k_1 - k_2 = \frac{\nu_1 - \nu_2}{c} + \frac{\nu_1 - \omega_{ab}}{V_g}. \quad (11)$$

The signal field $\Omega_4$ is generated by the polarization $\rho_{db}$ of the transition it couples [Eq. (8)]. The equation of motion for this polarization element reads

$$\dot{\rho}_{db} = -\Gamma_{db}\rho_{db} + i\Omega_4(\rho_{dd} - \rho_{bb}) - i\rho_{cb}\Omega_3, \quad (12)$$

where $\Gamma_{db} = \gamma_{db} + i(\omega_{db} - \nu_4)$, and $\nu_4$ is the frequency of generated field. In the steady-state regime and for $|\Omega_4| \ll |\Omega_3|$, the field $\Omega_4$ at the output of the cell is given by

$$\Omega_4 = -i\frac{\eta_4 e^{ik_4 L}}{\Gamma_{db}}\int_0^L dz e^{i(k_3-k_4)z}\rho_{cb}\tilde{\Omega}_3, \quad (13)$$

where $L$ is the length of the cell. Note here that Eq. (13) is valid if the field $|\Omega_3|$ does not affect the coherence $\rho_{cb}$ via power broadening which is true if $|\Omega_3|^2 \ll |\Omega_1|^2 + |\Omega_2|^2$.

Hence, after integrating Eq. (13), by using $\rho_{ab}$, $\rho_{ca}$, and $\rho_{bc}$ from Eqs. (9) and (10), we obtain for the scattered field $\Omega_4$

$$|\Omega_4|^2 = \left[\frac{\sin(\delta kL)}{\delta kL}\right]^2 \frac{\eta_4^2 L^2 |\Omega_1|^2 |\Omega_3|^2}{|\Gamma_{db}|^2 |\Omega_2|^2}, \tag{14}$$

where $\delta k = k_3 + \Delta k - k_4$, and the expression in the brackets describes the phase matching and determines the direction in which the signal field is generated (a small mismatch $\delta k$ of the order of $1/L$ is allowed).

The most interesting effect following from Eq. (14) is the coherent backscattering. Indeed, even when all three input fields propagate forward, one may observe a backscattered signal field by satisfying the condition

$$k_3 + \Delta k = k_3 + \frac{\omega_{cb}}{c} + \frac{\nu_1 - \omega_{ab}}{V_g} = -|k_4|, \tag{15}$$

and for appropriate detuning, $\nu_1 - \omega_{ab} < 0$, this equality can be met. That is, in order to obtain phase matching in the backward direction, we have to satisfy

$$-\frac{\nu_1 - \omega_{ab}}{V_g} = k_3 + \frac{\omega_{cb}}{c} + |k_4| \simeq 2|k_4|. \tag{16}$$

Hence, in order to demonstrate the effect, the detuning $\delta$ should meet the condition $\delta = -2|k_4|V_g$. It is useful to rewrite the condition in terms of susceptibility for the probe field, indeed,

$$k_1 = \frac{\nu_1}{c} n_1 \simeq \frac{\nu_1}{c}\left(1 + c\frac{\nu_1 - \omega_{ab}}{\nu_1 V_g}\right) = \frac{\nu_1}{c}\left(1 - c\frac{2|k_4|}{\nu_1}\right), \tag{17}$$

then, $\chi_{ab} = 2(n_1 - 1) = -4\frac{\lambda_{ab}}{\lambda_{db}}$, for gases $\chi_{ab} \ll 1$, so $\lambda_{ab} \ll \lambda_{db}$, i.e., the effect can be implemented for scattering of ir fields. Then, for the Doppler broadened EIT media as shown in [24,25], we can write

$$\chi_{ab}(\delta) \simeq \frac{3\lambda_{ab}^3 N}{8\pi^2}\left(\frac{\gamma_r \delta}{|\Omega_2|^2} + i\frac{\gamma_r \Delta_D \delta^2}{|\Omega_2|^4}\right), \tag{18}$$

where $\Delta_D = k_1 u_D$ is the Doppler width; $u_D$ is the rms velocity; $\gamma_r$ is the radiative decay rate. Thus, for detuning smaller than the EIT width $|\delta| \le |\Omega_2|^2/\sqrt{\gamma_r \Delta_D}$, absorption can be neglected, and

$$\frac{3\lambda_{ab}^2 N \gamma_r \delta}{16\pi |\Omega|^2} = -2|k_4|, \tag{19}$$

then, the atomic or molecular density is given by

$$N = \frac{32\pi|k_4|}{3\lambda_{ab}^2}\frac{|\Omega_2|^2}{\gamma_r|\delta|} \simeq \frac{32\pi|k_4|}{3\lambda_{ab}^2}\sqrt{\frac{\Delta_D}{\gamma_r}}. \tag{20}$$

There are several schemes to demonstrate the effect. For example, the double-Lambda scheme can be implemented in molecular rotational levels [see Fig. 1(a)]. Moreover, the effect can be implemented in the ladder-$\Lambda$ using molecular vibrational levels [see Fig. 3(a)]. The phase-matching condition should be slightly modified for this scheme as $k_4 = k_1 - k_2 - k_3$. Also, the phenomenon can be demonstrated in a $V$-$\Lambda$ scheme that can be realized in atomic levels [see Fig. 3(b), for Rb atoms, $b = 5S_{1/2}$, $c = 7D_{3/2,5/2}$, $a = 5P_{1/2,3/2}$, $d = 8P_{1/2,3/2}$], and phase-matching condition has a form $k_4 = k_1 + k_2 - k_3$. Let us note that the requirement for detuning in all cases is $\delta/V_g = -2|k_4|$, and the Eq. (20) to estimate molecular or atomic density is still valid.

As examples of systems where this effect could be observed, we suggest NO molecules (resonant transition at 236 nm, $A^2\Sigma^+ - X^2\Pi$), $NO_2$ molecules (resonant transition at wavelength 337 nm), and atomic Rb vapor. Let us note that EIT and CPT on molecules have been demonstrated recently, see [26]. The required molecular density of NO and $NO_2$ molecules is $N \simeq 1.2 \times 10^{13}$ cm$^{-3}$ if one can use transition between rotational levels $\simeq 10$ cm$^{-1}$. Using vibrational ir transitions for NO (vibration frequency of 1900 cm$^{-1}$) at 5.26 $\mu$m and for $NO_2$ (vibrational frequency of 750 cm$^{-1}$) 13.3 $\mu$m, the densities are $N = 8 \times 10^{15}$ cm$^{-3}$ and $N = 1.4 \times 10^{15}$ cm$^{-3}$, correspondingly. For atomic Rb vapor, wavelengths are $\lambda_1 = 780$ nm, $\lambda_2 = 565$ nm, $\lambda_3 = 335$ nm, $\lambda_4 = 23.4$ $\mu$m, and the atomic density is $N = 1.4 \times 10^{13}$ cm$^{-3}$.

The intensity needed for EIT is determined by the condition $|\Omega|^2 \gg \gamma_{bc}\Delta_D$ [24,25,27] which corresponds to a laser intensity of the order of 1 mW/cm$^2$ for atoms and of the order of 10 W/cm$^2$ for molecules, since typically the dipole moments are 2 orders of magnitude smaller for molecules. These conditions are realistic and well suited for an experimental implementation. We note that, for the schemes shown in Fig. 1(b) and 3(a), the coherence preparation fields, $\Omega_1$ and $\Omega_2$, are in a $\Lambda$ configuration and have almost the same frequency ($\nu_1 \simeq \nu_2$) hence there is no Doppler broadening on the TWO-photon transition [1,2]. Meanwhile, for the scheme shown in Fig. 3(b), the field

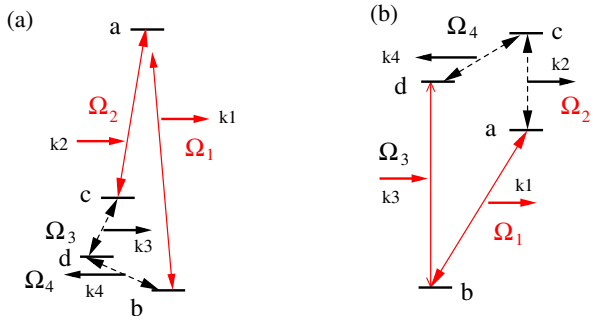


FIG. 3 (color online). Implementation: molecular systems, (a) vibrational levels; copropagating fields 1 and 2 induce coherent between vibrational levels. The field 3 propagating in the same direction will be scattered in the opposite direction. (b) Atomic Rb scheme for implementation of coherent backscattering.

frequencies are different, and the Doppler broadening at the two-photon transition leads to the depletion of the signal field $\Omega_1$ [21]. Then, Eq. (14) can be rewritten as

$$|\Omega_4|^2 = \frac{(1 - e^{-\kappa L})^2 + 4e^{-\kappa L}\sin^2\frac{\delta k L}{2}}{\delta k^2 + \kappa^2} \frac{\eta_4^2 |\Omega_1|^2 |\Omega_3|^2}{|\Gamma_{db}|^2 |\Omega_2|^2},$$

where $\kappa = 3\lambda^2 N \gamma_r (\gamma_{cb} + |\Delta k| u_D)/(8\pi|\Omega_2|^2)$ is the absorption coefficient of $\Omega_1$. One can see that the signal generation occurs at the effective length determined by the absorption of the signal field $L_{\text{eff}} = \kappa^{-1}$ instead of $L$. To avoid additional Doppler broadening, the experiments could be performed in cold gases.

Several applications of the effect can be envisioned, like in nonlinear CARS microscopy [28], while the controlling of coherent backscattering could provide a new tool for creating an image. A variation in the molecular density would modify the intensity of the signal in both the forward and the backward direction. Additionally, Eq. (14) also allows one to control the direction of the generated signal field and thus provide an all-optical control when scanning an optical field over an object.

In conclusion, we theoretically predict strong coherent scattering in the backward direction while using only forward propagating fields. This is achieved by exciting atomic or molecular coherence by properly detuned fields, in such a way that the resulting coherence has a spatial phase corresponding to a backward, counterpropagating wave. Applications of the technique to coherent scattering and remote sensing are discussed. The method holds promise for observing induced scattering in a backward direction with application to CARS microscopy.

We thank J. Giordmaine, K. Hakuta, N. Kroó, G. Kurizki, K. K. Lehmann, R. Miles, H. Walther, and X. S. Xie for useful discussions and gratefully acknowledge the support from the Defense Advanced Research Projects, the Office of Naval Research under Grant No. N00014-03-1-0385, the Robert A. Welch Foundation (Grant No. A1261).

[1] E. Arimondo, in *Progress in Optics*, edited by E. Wolf (Elsevier, New York, 1996), Vol. XXXV, p. 257; S. E. Harris, Phys. Today **50**, No. 7, 36 (1997).
[2] M. O. Scully and M. S. Zubairy, *Quantum Optics* (Cambridge University Press, Cambridge, England, 1997).
[3] S. E. Harris, Phys. Rev. Lett. **85**, 4032 (2000).
[4] A. B. Matsko, Yu. V. Rostovtsev, H. Z. Cummins, and M. O. Scully, Phys. Rev. Lett. **84**, 5752 (2000).
[5] A. B. Matsko, Y. V. Rostovtsev, M. Fleischhauer, and M. O. Scully, Phys. Rev. Lett. **86**, 2006 (2001).
[6] S. H. Harris, G. Y. Yin, M. Jain, and A. J. Mariam, Phil. Trans. R. Soc. A **355**, 2291 (1997).
[7] A. J. Merriam, S. J. Sharpe, M. Shverdin, D. Manuszak, G. Y. Yin, and S. E. Harris, Phys. Rev. Lett. **84**, 5308 (2000).
[8] H. Wang, D. Goorskey, and M. Xiao, Phys. Rev. Lett. **87**, 073601 (2001).
[9] R. Coussement, Y. Rostovtsev, J. Odeurs, G. Neyens, H. Muramatsu, S. Gheysen, R. Callens, K. Vyvey, G. Kozyreff, P. Mandel, R. Shakhmuratov, and O. Kocharovskaya, Phys. Rev. Lett. **89**, 107601 (2002).
[10] A. B. Matsko, O. Kocharovskaya, Y. Rostovtsev, G. R. Welch, A. S. Zibrov, and M. O. Scully, *The Advances in Atomic, Molecular, and Optical Physics*, edited by B. Bederson and H. Walther (Academic, New York, 2001), Vol. 46, p. 191.
[11] A. V. Turukhin, V. S. Sudarshanam, and M. S. Shahriar *et al.*, Phys. Rev. Lett. **88**, 023602 (2001).
[12] L. V. Hau, S. E. Harris, Z. Dutton, and C. H. Behroozi, Nature (London) **397**, 594 (1999).
[13] M. M. Kash, V. A. Sautenkov, A. S. Zibrov, L. Hollberg, G. R. Welch, M. D. Lukin, Y. Rostovtsev, E. S. Fry, and M. O. Scully, Phys. Rev. Lett. **82**, 5229 (1999); D. Budker, D. F. Kimball, S. M. Rochester, and V. V. Yaschuk, Phys. Rev. Lett. **83**, 1767 (1999).
[14] C. Y. Ye, A. S. Zibrov, Yu. V. Rostovtsev, and M. O. Scully, Phys. Rev. A **65**, 043805 (2002).
[15] V. A. Sautenkov, Y. V. Rostovtsev, H. Chen, P. Hsu, G. S. Agarwal, and M. O. Scully, Phys. Rev. Lett. **94**, 233601 (2005).
[16] H. Xiong, M. O. Scully, and M. S. Zubairy Phys. Rev. Lett. **94**, 023601 (2005).
[17] M. O. Scully, Phys. Rev. Lett. **55**, 2802 (1985); M. O. Scully and M. S. Zubairy, Phys. Rev. A **35**, 752 (1987).
[18] W. Schleich, M. O. Scully, and H.-G. von Garssen, Phys. Rev. A **37**, 3010 (1988); W. Schleich and M. O. Scully, Phys. Rev. A **37**, 1261 (1988).
[19] M. Jain, H. Xia, G. Y. Yin, A. J. Merriam, and S. E. Harris, Phys. Rev. Lett. **77**, 4326 (1996).
[20] M. O. Scully, G. W. Kattawar, P. R. Lucht, T. Opatrny, H. Pilloff, A. Rebane, A. V. Sokolov, and M. S. Zubairy, Proc. Natl. Acad. Sci. U.S.A. **99**, 10 994 (2002).
[21] Z. E. Sariyanni and Y. Rostovtsev, J. Mod. Opt. **51**, 2637 (2004).
[22] G. Beadie, Z. E. Sariyanni, Y. V. Rostovtsev, T. Opatrny, J. Reintjes, and M. O. Scully, Opt. Commun. **244**, 423 (2005).
[23] R. W. Boyd, *Nonlinear Optics* (Academic, New York, 1992).
[24] A. B. Matsko, D. V. Strekalov, and L. Maleki, Opt. Express **13**, 2210 (2005).
[25] H. Lee, Y. Rostovtsev, C. J. Bednar, and A. Javan, Appl. Phys. B **76**, 33 (2003).
[26] J. Qi, F. C. Spano, T. Kirova, A. Lazoudis, J. Magnes, L. Li, L. M. Narducci, R. W. Field, and A. M. Lyyra, Phys. Rev. Lett. **88**, 173003 (2002); J. Qi and A. M. Lyyra, Phys. Rev. A **73**, 043810 (2006).
[27] Y. Rostovtsev, I. Protsenko, H. Lee, and A. Javan, J. Mod. Opt. **49**, 2501 (2002).
[28] J. X. Cheng, A. Volkmer, and X. S. Xie, J. Opt. Soc. Am. B **19**, 1363 (2002).